Nanoscale

RSC Publishing

PAPER

View Article Online
View Journal

New optical method for enhanced detection of colon cancer by capsule endoscopy

Cite this: DOI: 10.1039/c3nr02396f

Rinat Ankri,†[a] Dolev Peretz,†[a] Menachem Motiei,[a] Osnat Sella-Tavor[b] and Rachela Popovtzer*[a]

PillCam®COLON capsule endoscopy (CE), a non-invasive diagnostic tool of the digestive tract, has dramatically changed the diagnostic approach and has become an attractive alternative to the conventional colonoscopy for early detection of colorectal cancer. However, despite the significant progress and non-invasive detection capability, studies have shown that its sensitivity and specificity is lower than that of conventional colonoscopy. This work presents a new optical detection method, specifically tailored to colon cancer detection and based on the well-known optical properties of immune-conjugated gold nanorods (GNRs). We show, on a colon cancer model implanted in a chick chorioallantoic membrane (CAM), that this detection method enables conclusive differentiation between cancerous and normal tissues, where neither the distance between the light source and the intestinal wall, nor the background signal, affects the monitored signal. This optical method, which can easily be integrated in CE, is expected to reduce false positive and false negative results and improve identification of tumors and micro metastases.

Received 9th May 2013
Accepted 27th July 2013

DOI: 10.1039/c3nr02396f

www.rsc.org/nanoscale

1 Introduction

Colon cancer is the third leading cause of cancer-related death in developing countries.[1,2] Despite major advances in treatment and therapy, early detection remains a key factor in increasing chances for successful treatment and ultimate cure.[3] Therefore, healthcare systems around the world recommend a routine colon cancer screening for people over the age of 50. Colonoscopy, which is currently the leading colon cancer screening method, is an endoscopic medical procedure that uses a small camera attached to a flexible tube, which when inserted into the rectum can reach and examine the entire length of the colon.[4] Although highly effective, this procedure can be painful and carries associated risks, such as injury to the intestinal wall, infection and internal bleeding. In addition, colonoscopies are usually avoided by patients due to the associated discomfort involved, the inconvenience of preparation, and other psychological inhibitions. In order to overcome these obstacles and decrease the potential pain and risk, Given Imaging (Yoqneam, Israel) has developed the PillCam®COLON capsule endoscopy (CE) which offers direct visualization of the colon in a non-invasive and painless way.[5,6] When ingested, this capsule, which is in the size and shape of a pill and contains a wireless camera, takes images of the inside of the gastrointestinal tract, which are then sent to a data recorder worn by the patient. In addition to detecting the esophagus and the colon, which can be seen using other types of endoscopy such as colonoscopy or esophagogastroduodenoscopy (EGD), the primary use of capsule endoscopy is to examine those areas of the small intestine that cannot be seen using conventional methods. However, despite the significant progress and non-invasive detection capability offered by the PillCam, studies have shown that its sensitivity is lower than that of conventional colonoscopy.[7,8]

In recent years, gold nanoparticles (GNPs) have become mainstay contrast agents for molecular imaging of cancer, mainly due to their ability to scatter and greatly enhance the reflection of the irradiated light in their surface plasmon resonance (SPR) frequency.[9,10] Using light scattering imaging techniques, several studies have demonstrated that cancer cells can be distinguished from normal cells based on the strong resonant light scattering of GNPs that specifically bind to cancer cells, as opposed to the random distribution and low intensity of nanoparticles around normal healthy cells.[11–13] However, distinction between cancerous and normal tissues based on differences in light intensity cannot be a reliable diagnostic tool suitable for colonoscopy and PillCam technology, since the distance between the light source and the colon tissue cannot be controlled. In PillCam technology, the capsule (light source and camera) freely cruises through the gastrointestinal tract. When adjacent to the intestinal wall, high light intensity can be detected even for a few randomly spread GNPs on healthy tissue, while weak light intensity can be detected when the capsule is far from the intestinal wall, even when large amounts of nanoparticles have accumulated on tumorous tissue.

[a]Bar-Ilan University, Faculty of Engineering & Institute of Nanotechnology & Advanced Materials, Ramat Gan 52900, Israel. E-mail: rachela.popovtzer@biu.ac.il
[b]Given Imaging LTD., Yoqneam, Israel
† Equally contributed

In order to resolve this issue, we have developed a novel optical detection method, specifically tailored to colon cancer detection. This detection method, based on the well-known optical properties of immune-conjugated GNPs, enables better differentiation between cancerous and normal tissues, where neither the distance between the light source and the intestinal wall, nor the background signal will affect the monitored signal. This optical method is expected to reduce false positive and false negative results, and could potentially be integrated in colonoscopy or PillCam technology.

The proposed method is based on the detection of the reflected light from the colon surface at three distinct wavelengths, which are separated by 20–50 nm and chosen according to the GNP extinction peak: the first wavelength is correlated with one of the wavelengths at the bottom of the peak, the second, at the full width half maximum (FWHM) of the peak, and the third is correlated with the peak wavelength (Fig. 1(a)). Using this method, the typical reflectance spectrum of cancerous tissues, while being conjugated with specifically targeted GNPs is expected to vary and to present the unique spectrum characteristics of GNPs. Since GNPs present a trend of increase within the three detected wavelengths, the specifically targeted cancer tissue is expected to follow the same pathway and to present the same increasing trend. In addition, as the GNPs are not present in non-cancerous tissues, the typical spectrum of the normal tissue is expected to be retained, and to present a constant or decreasing trend within the three detected wavelengths. Using this detection method, the absolute detected intensity becomes normalized and the distinction between cancerous and normal cells is based solely on the trend of the reflected light.

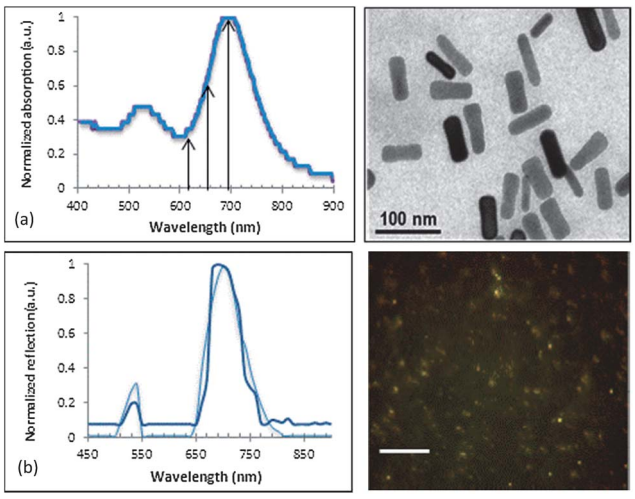

Fig. 1 Optical properties of the GNRs. (a) Left panel: normalized absorption spectrum of 25 × 75 nm GNRs. The three presented arrows point to the chosen wavelengths in this experiment. From left to right: 610, 650 and 690 nm. Right panel: TEM picture of bare GNRs. (b) Left panel: normalized scattering properties of bare GNRs (light blue) and CC49 bio conjugated GNRs (dark blue). Right panel: dark field microscopy of bare GNRs. The scattering properties were extracted from dark field images of the GNRs captured by the CCD camera of the hyper spectral microscopy. Scale bar is 10 μm.

2 Experimental

Two types of experiments are presented in this paper: a free-space optical setup for reflectance measurements of tissue-like phantoms, and a spectral microscopy setup for reflectance measurements of thin tissue sections. The free-space reflectance setup enables the collection of the total reflected light, which is composed of both the diffuse reflected light from thick tissue-like phantoms (with and without GNPs) and the surface reflected light (mainly due to backscattered light from GNPs). The second type of experiment is spectral microscopy measurement, which is performed in order to investigate the optical properties and spectral trend obtained from irradiated cancerous tissues targeted with GNPs, throughout the visible-NIR spectrum.

2.1 Gold nanorod (GNR) synthesis and bio conjugation

Gold nanorods (GNRs) were utilized as targeted contrast agents since they present the highest scattering properties compared to gold nanoshells or gold nanospheres.[14] The GNRs were synthesized using the seed mediated growth method.[15] Their size, shape and uniformity were characterized using transmission electron microscopy (TEM). The resultant average shape was 25 × 75 nm, with narrow size distribution (10%). The GNR extinction coefficient spectrum was determined using a spectrophotometer, and the resultant extinction peak was 690 nm (Fig. 1(a)).

In order to prevent aggregation, and to stabilize the particles in physiological solutions, a layer of polyethylene glycol (mPEG–SH, MW 5 000 g mol^{-1}) (creative PEGWorks, Winston Salem, USA) was adsorbed onto the GNRs. This layer also provided the chemical groups that are required for antibody conjugation (SH–PEG–COOH, MW 3400 g mol^{-1}). A solution of GNRs suspended in cetyltrimethylammonium bromide (CTAB) (Sigma-Aldrich, USA) was centrifuged at 11 000*g* for 10 min, decanted and resuspended in water to remove excess CTAB. A 200 μl mixture of mPEG–SH (5 mM) (85%) and SH–PEG–COOH (1 mM) (15%) was added to 1 ml of GNR solution. The mixture was stirred for 24 hours at room temperature. The absorption spectrum of PEGylated GNR solution presented the same absorption peak at 690 nm. For cancer cell targeting (LS174T), the heterofunctional PEG was covalently conjugated to a CC49 monoclonal antibody, which is specific to the TAG-72 antigen expressed in human colon cancer cells.[16]

2.2 *In vitro* cell binding experiment

A quantitative cell binding study was performed on LS174T and SW480 cells (2.5×10^6 each) in 5 ml DMEM medium containing 5% FCS, 0.5% penicillin and 0.5% glutamine (each experimental group was run in triplicate). Both cell types were incubated with 50 μl of CC49 coated GNRs (~10 mg ml^{-1}) for 10 minutes at 37 °C. After incubation, the medium was washed twice with PBS followed by the addition of 1 ml of aqua regia HCl : HNO_3 (1 : 3) (Sigma-Aldrich). After evaporation of the acid, the sediment was dissolved in 5 ml 0.05 M HCl. The gold concentrations of the samples were quantified by Atomic Absorption Spectroscopy (AA 140; Agilent Technologies, Santa Clara, CA).

2.3 Macro free-space optical setup

An optical setup was designed and built (Negoh-Op Technologies, Israel) for free-space reflected light intensity measurements.[17,18] The set-up includes a laser diode with a wavelength of 650 nm as an excitation source. The irradiation was carried out using an optic fiber with a diameter of 125 μm to achieve a pencil beam illumination. The irradiated light was collimated and the beam size on the sample was not larger than 500 μm. We used a portable photodiode as a photo detector. The photodiode had a cross-section diameter of 1 mm^2. The distance between the light source and the photodiode was ~1 mm. The total reflected intensity was collected using a digital scope (Agilent Technologies, Mso7034a, Santa Clara, CA).

2.4 Tissue-like solid phantoms

Solid phantoms were prepared in order to simulate human tissue optical properties.[19,20] The phantoms were prepared using India ink 0.1%, as an absorbing component and Intralipid (IL) 20% (Lipofundin MCT/LCT 20%, B. Braun Melsungen AG, Germany), as a scattering component.[21] Agarose powder 1% (SeaKem LE Agarose, Lonza, USA) was added in order to convert solution into gel. All phantoms presented the same absorption and reduced scattering coefficients (0.01 mm^{-1} and 1.5 mm^{-1}, respectively), using 1% of India ink and 2% of IL (this concentration refers to the solid fraction in the examined solution). Two types of phantoms were prepared. Both types presented identical concentrations of ink and IL. Into one type of phantoms, 100 μl of GNPs (25 mg ml^{-1}) were added to simulate a tissue containing GNPs. The solutions were heated and mixed at a temperature of approximately 90 °C while the Agarose powder was slowly added. The phantom solutions were then poured into cell culture plates (90 mm) and cooled under vacuum conditions. All phantoms were 15 mm in thickness.

2.5 Chorioallantoic membrane model (CAM)

In this research, a chick embryo chorioallantoic membrane (CAM) has been chosen as a model system for colon cancer. The CAM model is a borderline case between *in vivo* and *in vitro* systems, and is ideal for our study since it closely imitates colon cancer characteristics. In colon cancer, tumors develop partly inside the colon tissue and partly on the intestinal wall bulging outward. Likewise, in the CAM model, tumors develop in the same manner, with the tumor partially inside the egg membrane and partially on the membrane surface bulging outward.[22,23] The CAM is a transparent and highly vascularized membrane, formed during embryo development on day 4 to 5, by the fusion of the mesodermal layers of both the allantois and the chorion,[24–26] resulting in a highly vascularized mesoderm composed of arteries, veins, and an intricate capillary plexus.[27] The developing embryo is naturally immunodeficient, therefore the CAM is an excellent host for cancer cells biopsied from patients, and is extremely accessible to experimental manipulation. Tumors grafted on the CAM surface have characteristics similar to those grown in mammalian models. Compared with mammalian models, the CAM method exhibits faster tumor growth, low cost, simplicity, and does not require government approval.

Two types of colon cancer cells have been implanted in the CAM model: LS174T which highly over expresses the TAG-72 antigen, and SW480 which has only minor expression of TAG-72. GNRs are coated with the CC49 antibody, for specific targeting of the LS174T cells.[14,28] Using hyper spectral microscopy, the reflectance intensity was measured for the normal tissue, the control tissue (grown from SW480 after incubation with CC49 coated GNRs) and the specifically targeted colon cancer tissue (grown from LS174T and targeted with CC49 coated GNRs).

Fertilized eggs from Lohman-selected white leghorn chickens were incubated for 3 days at 37 °C in 60% relative air humidity and rotated hourly. On day 3 of incubation, a rectangular window (1–1.5 cm) was made in the eggshell. Two milliliters of albumen were withdrawn using a 21-gauge needle through the large blunt end of the egg. The window was covered with a piece of tape to prevent dehydration, and the eggs were replaced in the incubator. On day 8 of incubation, 5×10^5 LS174T or SW480 colon cancer cells were grafted to the CAM under sterile conditions. The cells were placed within a very thin, 5 mm diameter plastic ring that was deposited on top of a blood vein intentionally damaged using a needle. The damaged vein supplied oxygen to the cancer cells, enabling tumor development. Four days post-cell implantation, the eggs were reopened and the tumor was extracted for cancer detection experiments. Images of the tumor tissue inside and outside of the egg are presented in Fig. 2 (left and right panels, respectively).

For GNR targeting experiments, a droplet of 15 μl of CC49 bio conjugated GNRs (3 mg ml^{-1}) was placed on the tumor in the egg and incubated for 10 min, after which the tumor was washed with PBS to remove excess GNRs (not attached to the cells). The tumor was then extracted from the egg and the reflected signal was measured using hyper spectral microscopy.

2.6 Hyper spectral imaging system

Reflectance measurements of GNRs and cancerous tissues were captured using the hyper spectral imaging system (Nuance, CRi, MA, USA). A Halogen illumination (UN2-PSE100, Nikon, Japan), along with 40× objective (0.75 NA) and a 32 bit ultrasensitive CCD camera detector (N-MSI-EX), was used for imaging in RGB

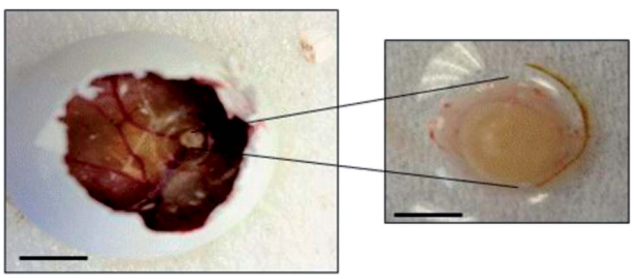

Fig. 2 Chick embryos in shell-less culture *ex vivo*. The left panel of the picture presents images depicting an 11-day chick embryo. The right panel of the figure presents the colon tumor extracted from the egg. Scale bars are 30 mm (left panel) and 6.5 mm (right panel).

mode. Microscopy was then performed with a Nikon 80i Microscope (Nikon Instruments, Inc.). Images were acquired using the Nuance software version 2.1.

As the tumor surface was not flat, a captured image introduced areas in focus as well as areas out of focus. For each spectral analysis, three regions of interest (ROIs) from the tumor picture were chosen, each presenting the largest region in focus.

The effect of the backing material on the reflectance signal from the cancerous colon tissue was studied. The colon tissue (LS174T and SW480) was placed on a thin embryonic tissue (few millimeters in thickness), on a slice of chicken ham, on a black paper and on a glass slide. Measurements have demonstrated that the reflectance signal from the tumor tissue was not affected by the backing material (results not shown). Therefore, a thin embryonic tissue was used in all measurements.

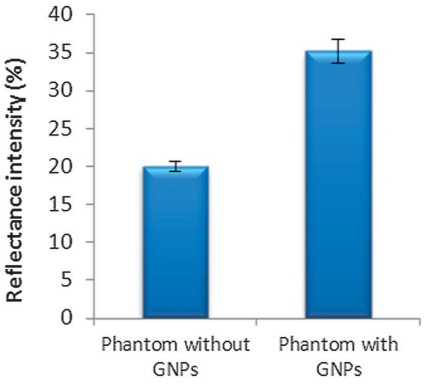

Fig. 3 A comparison between the reflectance intensity of phantoms with and without GNPs. The intensity of the reflected light from phantoms with GNPs is over 1.75 times higher than that from phantoms without GNPs. Three independent measurements were performed and the error bars represent the error of the mean. The results are presented as the percentage of the illumination intensity.

3 Results and discussion

3.1 *In vitro* cell binding experiment

To evaluate the specificity of the interaction between the CC49 coated GNRs and the LS174T colon cancer cells, the GNRs were introduced to the LS174T cells and to the control SW480 cells. Flame atomic absorption spectroscopy measurements quantitatively demonstrated that the interaction between the CC49 coated GNRs and the LS174T cells was significantly more specific than the interaction of the GNRs with the SW480 cells. The LS174 cells took up 2.66×10^3 GNRs per cell while SW480 cells absorbed only 1.04×10^2 GNRs per cell. These results correlate well with previously published studies, which report that LS174T cells highly express the TAG-72 antigen.[29,30]

3.2 Free-space reflectance measurements

Free-space reflectance measurements[31] were performed in order to investigate whether the reflectance intensity from GNPs does overcome the background signal (the diffuse reflected light from the surrounding illuminated colon tissue). Two types of phantoms were measured: the first, phantoms without GNPs and the second, phantoms with 2.5 mg of GNPs. The phantoms were illuminated with 650 nm wavelength and the total reflectance intensity (1 mm from the illumination source) was measured. The results clearly show that the intensity of the reflected light from phantoms with GNPs is over 1.75 times higher than that from phantoms without GNPs (see Fig. 3). These results demonstrate that the intensity of the reflected light from GNPs overcomes the inevitable diffuse light intensity from the surrounding illuminated tissue and thus pave the way for our next *in vitro* measurements of the reflected signal from colon cancer tissue decorated with CC49 bio-conjugated GNRs.

3.3 Spectral microscopy measurements

In order to investigate the spectral difference between cancer tissues labeled specifically (LS174T) and non-specifically (SW480) by the CC49 coated GNRs, their reflectance signals have been measured along the entire visible-NIR spectrum (450–900 nm) after 10 min of incubation with CC49 coated GNRs. Incubation of 10 min was chosen in order to enable the GNR attachment to the cancer cell surface and yet to avoid their endocytosis, which might decrease their reflectance intensity.[32,33] In an *in vivo* application, GNRs will be directly inserted to the colon, in order to protect the antibodies from stomach acid.

Fig. 4(a) shows representative normalized spectra of the total reflected light from the sample, composed of both the diffuse reflected light from the tissue and the backscattered light from GNRs. As demonstrated, there is a clear difference between the two samples, as the specifically targeted LS174T tissue presents higher total reflectance light intensity (normalized) as well as a broadening towards the red region, in comparison to SW480. Both differences indicate the presence of large amounts of GNRs in the LS174T targeted tissue, while only small amounts of GNRs were attached non-specifically to the SW480. These

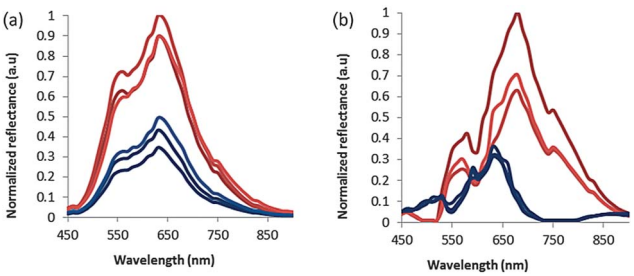

Fig. 4 Normalized reflectance spectra. (a) A comparison between the normalized reflectance spectra of targeted LS174T (red colored lines) and non-targeted SW480 (blue colored lines) colon cancer tissue with CC49 bio conjugated GNRs. The normalized reflection from the LS174T is about three times higher than the total reflectance from SW480 cells, indicating the specific attachment of the GNRs to the cancer cells. (b) Normalized backscattered light intensity from the GNRs decorating the colon cancer tissue. The spectrum was obtained after the reduction of the background signal from the total reflectance signal (performed using the *Nuance* software). A spectrum of the tissue without GNRs was subtracted from the spectrum of the tissue with GNRs, to emphasize GNR attachment to the cells. For all samples, the backing material was a thin embryonic tissue, measuring a few millimeters in thickness. Spectra were normalized to the maximal intensity obtained.

results well correlate with our *in vitro* results presented in Section 3.1 above, demonstrating the higher affinity of the CC49 bio-conjugated GNRs to the LS174T cells.

Fig. 4(b) compares the normalized reflected light intensity from LS174T and SW480 colon cancer tissues following their incubation with CC49 GNRs. The reflected light from the tissue without GNRs (background signal) was reduced from the total reflectance. Three clear differences can be observed: (1) the LS174T tissue presents a spectral peak at 680 nm, similar to the GNRs, while the SW480 tissue shows a spectral peak at 640 nm, which is similar to the reflectance spectrum of the illuminating lamp (data not shown). (2) The spectral intensity peak of the specifically targeted LS174T tissue is over 3 times higher than that for the non-specifically targeted SW480 colon tissue. Since the backscattered light from GNRs correlates with the number of GNRs in the sample, the higher intensity from the LS174T indicates a 300% greater affinity of the CC49 coated GNR, to the LS174T cells than to the SW480 cells, using the same excitation conditions. (3) By comparing the normalized reflected light intensity of LS174T labeled with CC49 GNRs and that of the bare GNRs (presented in Fig. 1(b)), other than broadening of the spectrum, an additional smaller peak at ~750 nm can be observed. This suggests that the electromagnetic fields of adjacent nanoparticles overlap, resulting in a significant red-shift of the resonance wavelength peak of adjacent nanoparticles, unlike that of individual particles.[28,34,35] This red shift occurs only where high density GNRs specifically bind to the colon cancer cells *via* the CC49 antibody to their target epitope, while the non-targeted GNPs that might randomly spread in the colon will not present a spectral shift.[35]

3.4 Distance dependent reflectance intensity measurements

As mentioned in the Introduction, the colonoscopy and PillCam detection technologies cannot be based on the reflectance-intensity differences between cancerous and non-cancerous cells, since the intensity also changes in relation with the distance between the detector and the intestinal wall. Fig. 5 depicts the effect of the light source–detector distance on the detected intensity: when the vertical distance between the tissue and the detector of the hyper spectral imaging system decreases by 1.3 mm, the total reflectance intensity increases by 400%. This implies that the dominant factor determining the total reflectance intensity is the distance between the detector and the intestinal wall, rather than the density of the GNRs (which correlates with cancerous or non-cancerous tissue).

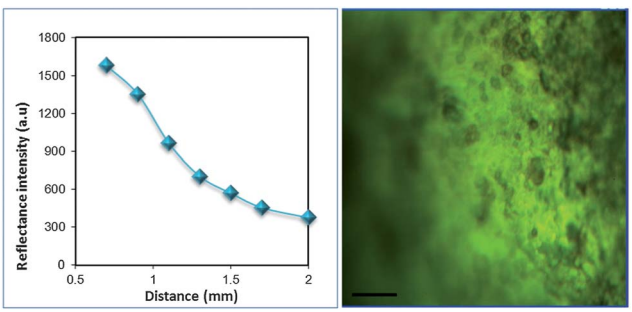

Fig. 5 The reflectance intensity of LS174T cells as was measured by multi wavelength irradiation using hyperspectral microscopy. Right panel: reflectance image of LS174T cells as captured by the hyper spectral camera. Left panel: dependence of the total reflectance intensity on the vertical distance from the tumor. Each point on the curve is the intensity for a given distance measured at the peak of the reflectance spectrum (at 650 nm). Scale bar is 10 μm.

3.5 Spectral trend

In order to overcome the distance-dependent intensity problem, the proposed detection technique provides the ability to identify the presence of GNRs by their unique spectral shape rather than their absolute high reflectance intensity. In this method, the tissue should be simultaneously irradiated with three distinct wavelengths (*e.g.* three distinct diode lasers) that could potentially be integrated in the colonoscope or the capsule. Since the distance of each of these diodes from the intestinal wall is identical for a given measurement, the trend (slope), rather than absolute intensity, can indicate the presence or absence of specifically targeted GNRs. Fig. 6 shows the different trends obtained from targeted (LS174T) and non-targeted (SW480) colon cancer tissues following conjugation with GNRs. The three wavelengths were chosen according to the extinction spectra of the GNRs (as shown in Fig. 1); 610 nm correlates with the bottom of the peak, 650 nm is similar to the FWHM of the peak, and 690 nm to the peak. As demonstrated, a decreasing trend (negative slope) was obtained from the normalized reflectance signal of the three wavelengths for the non-targeted tissue, correlating to the typical trend of tissues without GNRs (see Fig. 4(b)). In contrast, an increasing trend (positive slope) was obtained for the specifically targeted LS174T tissue, reflecting exactly the trend obtained by the GNRs. This unique increasing spectroscopic signal, which is distinct from the typical spectrum of normal tissues, denotes the presence of colon cancer cells.

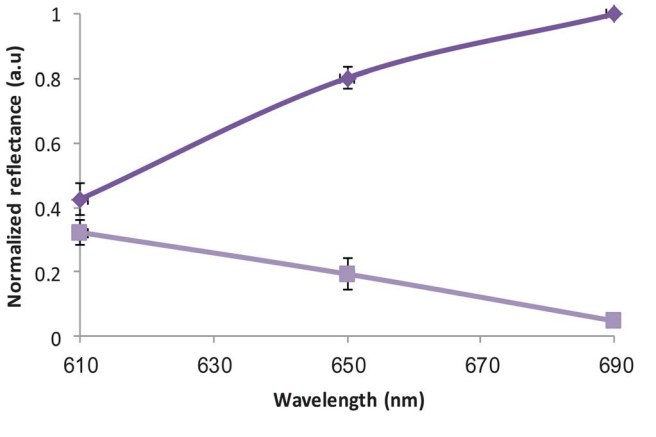

Fig. 6 A comparison between the backscattered light from targeted (LS174T) and non-targeted (SW480) colon cancer tissues following conjugation with GNRs. The three wavelengths were chosen according to the extinction spectra of the GNRs (as shown in Fig. 1). Diamond marked line: trend of normalized reflection for LS174T. Square marked line: trend of normalized reflection for SW480. The results are the average of different reflection measurements. The error bars represent error of the mean.

4 Conclusions

In summary, this study presents an innovative colon cancer detection method, which could be incorporated in conventional colonoscopy or the PillCam capsule technology. Simultaneous irradiation of colon tissues with three distinct diode lasers provides the ability to detect the presence of GNRs by their typical spectroscopic shape, rather than by their absolute intensity. The proven biosafety of GNRs *in vivo*,[36–38] along with the fact that the present application necessitates only topical rather than systemic administration, provides the potential for GNRs to become clinically approved in the near future. Together with the ability to specifically attach GNRs with high density to colon cancer cells, this technology is expected to provide a definitive discrimination between cancerous and normal tissues, and to reduce false positive and false negative results.

Acknowledgements

This work was supported by a Research and Development - Chief Scientist Nofar grant.

References

1 T. Byers, B. Levin, D. Rothenberger, G. D. Dodd and R. A. Smith, *Ca-Cancer J. Clin.*, 1997, **47**, 154–160.
2 Y. Kakugawa, Y. Saito, S. Saito, K. Watanabe, N. Ohmiya, M. Murano, S. Oka, T. Arakawa, H. Goto, K. Higuchi, S. Tanaka, H. Ishikawa and H. Tajiri, *World J. Gastroenterol.*, 2012, **18**, 2092–2098.
3 B. Levin, D. A. Lieberman, B. McFarland, R. A. Smith, D. Brooks, K. S. Andrews, C. Dash, F. M. Giardiello, S. Glick, T. R. Levin, P. Pickhardt, D. K. Rex, A. Thorson and S. J. Winawer, *Ca-Cancer J. Clin.*, 2008, **58**, 130–160.
4 J. A. Eaden, B. A. Ward and J. F. Mayberry, *Gastrointestinal Endoscopy*, 2000, **51**, 123–128.
5 N. Schoofs, J. Deviere and A. Van Gossum, *Endoscopy*, 2006, **38**, 971–977.
6 R. Eliakim, Z. Fireman, I. M. Gralnek, K. Yassin, M. Waterman, Y. Kopelman, J. Lachter, B. Koslowsky and S. N. Adler, *Endoscopy*, 2006, **38**, 963–970.
7 C. Spada, C. Hassan, R. Marmo, L. Petruzziello, M. E. Riccioni, A. Zullo, P. Cesaro, J. Pilz and G. Costamagna, *Clin. Gastroenterol. Hepatol.*, 2010, **8**, 516–522.
8 R. Eliakim, K. Yassin, Y. Niv, Y. Metzger, J. Lachter, E. Gal, B. Sapoznikov, F. Konikoff, G. Leichtmann, Z. Fireman, Y. Kopelman and S. N. Adler, *Endoscopy*, 2009, **41**, 1026–1031.
9 K. H. Su, Q. H. Wei, X. Zhang, J. J. Mock, D. R. Smith and S. Schultz, *Nano Lett.*, 2003, **3**, 1087–1090.
10 P. K. Jain, K. S. Lee, I. H. El-Sayed and M. A. El-Sayed, *J. Phys. Chem. B*, 2006, **110**, 7238–7248.
11 I. H. El-Sayed, X. Huang and M. A. El-Sayed, *Nano Lett.*, 2005, **5**, 829–834.
12 L. W. Chan, Y.-N. Wang, L. Y. Lin, M. P. Upton, J. H. Hwang and S. H. Pun, *Bioconjugate Chem.*, 2012, **24**, 167–175.
13 E. C. Dreaden and M. A. El-Sayed, *Acc. Chem. Res.*, 2012, **45**, 1854–1865.
14 P. K. Jain, K. S. Lee, I. H. El-Sayed and M. A. El-Sayed, *J. Phys. Chem. B*, 2006, **110**, 7238–7248.
15 B. Nikoobakht and M. A. El-Sayed, *Chem. Mater.*, 2003, **15**, 1957–1962.
16 K. S. Kim, Y. K. Lee, J. S. Kim, K. H. Koo, H. J. Hong and Y. S. Park, *Cancer Gene Ther.*, 2008, **15**, 331–340.
17 R. Ankri, H. Taitelbaum and D. Fixler, *J. Biomed. Opt.*, 2011, **16**, 085001–085006.
18 R. Ankri, V. Peretz, M. Motiei, R. Popovtzer and D. Fixler, *Int. J. Nanomed.*, 2012, **7**, 449–455.
19 J. S. Dam, C. B. Pedersen, T. Dalgaard, P. E. Fabricius, P. Aruna and S. Andersson-Engels, *Appl. Opt.*, 2001, **40**, 1155–1164.
20 C. Yaqin, L. Ling, L. Gang, Y. Wenyu and Y. Qilian, *IEEE Int. Conf. Neural Networks & Signal Processing*, 2003, vol. 1, pp. 369–372.
21 R. Cubeddu, A. Pifferi, P. Taroni, A. Torricelli and G. Valentini, *Phys. Med. Biol.*, 1997, **42**, 1971–1979.
22 D. Ribatti, *Int. Rev. Cell Mol. Biol.*, 2008, **270**, 181–224.
23 E. Corem-Salkmon, B. Perlstein and S. Margel, *Int. J. Nanomed.*, 2012, **7**, 5517–5527.
24 A. Cimpean, D. Ribatti and M. Raica, *Angiogenesis*, 2008, **11**, 311–319.
25 Y. Endo, M. Seiki, H. Uchida, M. Noguchi, Y. Kida, H. Sato, M. Mai and T. Sasaki, *Cancer Sci.*, 1992, **83**, 274–280.
26 D. F. Tucker and J. J. T. Owen, *Eur. J. Cancer*, 1969, **5**, 591–596.
27 M. Taizi, V. R. Deutsch, A. Leitner, A. Ohana and R. S. Goldstein, *Exp. Hematol.*, 2006, **34**, 1698–1708.
28 S. Mallidi, T. Larson, J. Aaron, K. Sokolov and S. Emelianov, *Opt. Express*, 2007, **15**, 6583–6588.
29 P. Zou, S. Povoski, N. Hall, M. Carlton, G. Hinkle, R. Xu, C. Mojzisik, M. Johnson, M. Knopp, E. Martin, Jr and D. Sun, *World J. Surg. Oncol.*, 2010, **8**, 1–13.
30 R. P. McGuinness, Y. Ge, S. D. Patel, S. V. Kashmiri, H. S. Lee, P. H. Hand, J. Schlom, M. H. Finer and J. G. McArthur, *Hum. Gene Ther.*, 1999, **10**, 165–173.
31 R. Ankri, V. Peretz, M. Motiei, R. Popovtzer and D. Fixler, *Int. J. Nanomed.*, 2012, **7**, 449–455.
32 J. C. Kah, K. W. Kho, C. G. Lee, C. James, R. Sheppard, Z. X. Shen, K. C. Soo and M. C. Olivo, *Int. J. Nanomed.*, 2007, **2**, 785–798.
33 J. Aaron, K. Travis, N. Harrison and K. Sokolov, *Nano Lett.*, 2009, **9**, 3612–3618.
34 S. Mallidi, T. Larson, J. Tam, P. P. Joshi, A. Karpiouk, K. Sokolov and S. Emelianov, *Nano Lett.*, 2009, **9**, 2825–2831.
35 R. Ankri, A. Meiri, S. I. Lau, M. Motiei, R. Popovtzer and D. Fixler, *J. Biophys.*, 2012, **6**, 188–196.
36 T. Niidome, M. Yamagata, Y. Okamoto, Y. Akiyama, H. Takahashi, T. Kawano, Y. Katayama and Y. Niidome, *J. Controlled Release*, 2006, **114**, 343–347.
37 M. Eghtedari, A. V. Liopo, J. A. Copland, A. A. Oraevsky and M. Motamedi, *Nano Lett.*, 2008, **9**, 287–291.
38 G. von Maltzahn, J.-H. Park, A. Agrawal, N. K. Bandaru, S. K. Das, M. J. Sailor and S. N. Bhatia, *Cancer Res.*, 2009, **69**, 3892–3900.

